



UNICA

UNIVERSITÀ  
DEGLI STUDI  
DI CAGLIARI



Università di Cagliari

UNICA IRIS Institutional Research Information System

**This is the Author's accepted manuscript version of the following contribution:**

Paolo Castello, Giacomo Gallus, Carlo Muscas, Paolo Attilio Pegoraro, Davide Sitzia, Sara Sulis

**A Statistical Investigation of PMU Errors in Current Measurements**

CONFERENCE PROCEEDINGS - IEEE INSTRUMENTATION/MEASUREMENT TECHNOLOGY CONFERENCE 2023

**The publisher's version is available at:**

<https://dx.doi.org/10.1109/i2mtc53148.2023.10175893>

**When citing, please refer to the published version.**

“© 2023 IEEE. Personal use of this material is permitted. Permission from IEEE must be obtained for all other uses, in any current or future media, including reprinting/republishing this material for advertising or promotional purposes, creating new collective works, for resale or redistribution to servers or lists, or reuse of any copyrighted component of this work in other works

# A Statistical Investigation of PMU Errors in Current Measurements

Paolo Castello, Giacomo Gallus, Carlo Muscas, Paolo Attilio Pegoraro, Davide Sitzia, Sara Sulis

*Department of Electrical and Electronic Engineering*

*University of Cagliari*

Cagliari, Italy

davide.sitzia@unica.it

**Abstract**—Phasor Measurement Units (PMUs) are becoming widespread in power systems monitoring. Applications relying on synchrophasor measurements ask for models of measurement errors that can be integrated to describe the uncertainty of the data. In this paper, an assessment of PMU magnitude and phase-angle errors for current measurements is performed for the first time with the aim to address error distributions. In particular, two commercial PMUs are statistically characterized in a controlled environment to prevent non-stationarity issues. It is proven that Gaussianity appears a valid assumption for magnitude errors of both PMUs, whereas phase-angle errors might be non-Gaussian in an accurate PMU when the contribution of synchronization mechanisms prevails.

**Index Terms**—Phasor Measurement Unit (PMU), measurement uncertainty, current measurement, Gaussianity test

## I. INTRODUCTION

Phasor Measurement Units (PMUs) are the key element for many advanced monitoring and control applications in the new generation power systems. They are currently installed in transmission systems, but an employment in distribution systems is also foreseen.

The PMU includes the signal conditioning, the acquisition system, the synchronization module, the computation stages where algorithms are applied and the communication module. All elements except the last one can be considered as a source of uncertainty in the measurement process. PMUs implement different algorithms and thus they can differ significantly from one another [1].

PMUs measure synchronized phasors of voltage and current signals and each measurement is timestamped with respect to the Coordinated Universal Time (UTC) through time synchronization capabilities integrated into the device [2].

Commercial PMUs should comply with the standard IEC/IEEE 60255-118-1 [3], which includes specifications on the maximum errors depending on the considered class (P or M), the specific test condition and the reporting rate. In particular, despite the fact that the Total Vector Error (TVE) is the main index for synchrophasor evaluation, a better representation of the PMU characteristics could be achieved by explicitly considering the two main elements of the TVE, i.e., magnitude and phase-angle errors. Synchronization errors, which can arise due to either internal or external causes, affect directly phase-angle errors and thus contribute to TVE.

Measurements from PMUs can be aligned thanks to the accurate timestamps and used to feed different kinds of applications [4]. Knowledge about the uncertainty associated to PMU measurements is important for any decision-making or optimization process. For instance, state estimation usually relies on measurements weighing based on the associated uncertainty [5]. To this aim, guaranteed compliance of TVE with respect to the standard limits is not enough and a more complete description would be advisable, possibly including realistic error models.

Error contributions can have either systematic or random nature. The former ones can be partially compensated, if estimated [6], whereas the latter, which are tied to unpredictable changes in the PMU behavior, can be modeled in some applications through their probability distribution [7]. PMU magnitude and phase-angle errors from a PMU device are typically assumed as normally distributed [8], [9] but recent literature indicates that non-Gaussian model might also be considered. In [10], voltage magnitude and phase-angle errors are found (based on field measurements) to follow long-tailed non-Gaussian distributions. In [7] non-Gaussian distribution also emerges for voltage errors from offline and online measurements.

In [11], a thorough statistical characterization of PMU voltage magnitude and phase-angle errors through laboratory experiments was carried out under controlled conditions so that a meaningful reference is always available and the impact of non-stationary conditions typical of field measurements can be excluded.

In this paper, following the same rigorous approach as in [11], an analysis of PMU errors in current measurements is performed. A controlled laboratory environment is used to keep the device under steady-state conditions, so that model inconsistencies due to non-stationary signals are clearly avoided, and different current levels are considered. Statistical tools are applied to the measurements, aiming at suggesting possible models for PMU-based applications involving also current measurements.

## II. PMU CHARACTERIZATION: TEST ARCHITECTURE AND CONFIGURATION

In this section, the test system used to assess PMU error characteristics is presented. In this study, for the sake of a more

detailed comprehension of the involved phenomena, the focus is on the behavior of the PMU device, while external instrument transformers (ITs), which may have great relevance in the whole synchrophasor measurement chain, are not considered in the analysis. In this context, ITs are often supposed to introduce systematic errors [12], [13], therefore their influence might be mainly on the average of the measurement chain errors. However, any IT characterization can be used together with that of PMU errors to better describe the overall behavior.

### A. Test System

The synchrophasor data have been collected from experimental tests conducted in the instrumentation and measurement laboratory of the University of Cagliari (Italy). Figure 1 shows the test architecture, which has been used to characterize two commercial PMUs (referred to as PMU 1 and PMU 2, respectively). PMU 1 is a commercial device equipped with a total of eight input channels for voltage and current acquisition. It features different full-scale ranges (FSRs): in the performed tests, the 240 V, 2.5 A and 5 A ranges are involved for voltage and current measurements, depending on the test. PMU 2 is equipped with voltage and current acquisition modules featuring respectively three and four input channels. FSRs of 300 V and 5 A characterize the two modules, respectively.

The high-accuracy power signal generator and calibrator Omicron CMC 256plus [14] is used to generate the three-phase steady-state current signals feeding the PMUs under test. Four different levels of current were considered to test the PMUs in different working conditions: 0.5 A, 1.0 A, 2.5 A and 5.0 A. The calibrator's accuracy is declared by the vendor as 0.015 % of reading plus 0.005 % of the device FSR, which can be set to either 1.25 A or 12.5 A. Typical phase-angle accuracy of the synchronized generation is  $8.7 \cdot 10^{-3}$  crad at 50 Hz. The use of the power signal calibrator allowed to test the PMUs

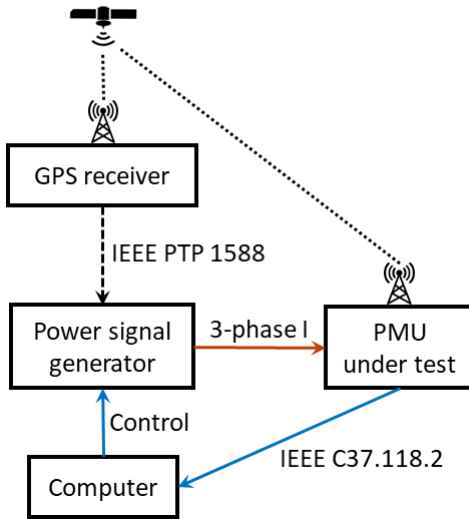


Fig. 1. Test architecture.

in known operating conditions through steady-state signals, in order to provide the relevant measurement error statistics.

The PMUs are configured to use a reporting rate of 50 frames per second (fps) and the generated IEEE C37.118.2 packets [15] are collected by an industrial computer, which is equipped with some Phasor Data Concentrator (PDC) functionalities, since it is in charge of TCP packets reception and decapsulation. The computer also stores synchrophasor data and sends the control signals used to configure the power signal generator and the PMUs.

The architecture includes a Meinberg Lantime M1000 GPS receiver, which provides the synchronization signal to the calibrator via IEEE 1588 protocol, configured in the power profile [16].

### B. Considered Metrics and Analysis

Figure 2 reports the block diagram of the considered analysis steps (software tools used for the developed routines are also indicated for each module).

As a preliminary step, the performance evaluation of synchrophasor current measurements for both PMUs was performed by computing the percent TVE as follows:

$$\text{TVE}(n) = 100 \cdot \frac{|\hat{I}(n) - \bar{I}(n)|}{I(n)} \quad (1)$$

where  $\hat{I}(n)$  is the measured current synchrophasor at instant  $n$  (corresponding to  $nT_s$ , with  $T_s = 20$  ms the reporting interval),  $\bar{I}(n)$  is its reference counterpart with magnitude  $I(n)$ . For low errors, the TVE index sums up in a quadratic way magnitude and phase-angle contributions, thus quantifying the deviation of the estimated phasor from the reference. The TVE is computed for each measurement  $n$  and its maximum value within the dataset corresponding to the test duration is recorded, in order to assess the compliance to the standard [3], which requires a maximum TVE  $< 1\%$  in steady-state conditions.

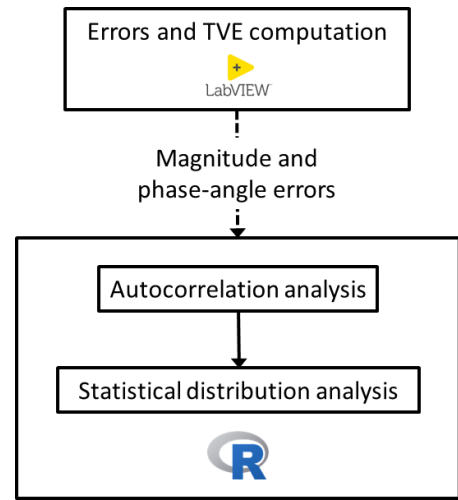


Fig. 2. Scheme of the analysis steps.

Magnitude and phase-angle errors are also considered as input of the following statistical analysis. Magnitude errors are evaluated in percentage, while the phase-angle errors are considered in absolute terms, as follows:

$$\text{ME}(n) = 100 \cdot \frac{\widehat{I}(n) - I(n)}{I(n)} \quad (2)$$

$$\text{PE}(n) = \angle \widehat{I}(n) - \angle I(n) \quad (3)$$

where  $\widehat{I}(n)$  is the magnitude of the measured synchrophasor and  $\angle$  denotes the phase angle of the corresponding synchrophasor.

The statistical analysis (developed in the RStudio [17] supporting the R programming language), whose main purpose is to identify whether the typology of the errors distribution from various tests could be considered Gaussian or not, was preceded by an offline post-processing procedure of the collected measurements, necessary to obtain the data subsequently examined.

An autocorrelation analysis of each measurement error set is performed as in [11], since it is essential for unmasking the possible presence of dependency in the data, which could make the results of the statistical analysis of little significance. Indeed, high autocorrelation values in a limited set of data can result in empirical distributions that are not very representative of the underlying statistical model. The statistical analysis is then performed through Shapiro-Wilk (S-W) test [18] applied to vectors of error samples that are characterized by low autocorrelation and are thus obtained, if necessary, by decimation from longer input vectors.

S-W test provides as output a numerical result, the  $p$ -value ( $p$ ), whose value determines the rejection or not of the null hypothesis, depending on the chosen significance level  $\alpha$ . An  $\alpha$  level equal to 0.05 was chosen, according to the scientific literature on PMU errors evaluation. In this paper the null hypothesis is represented by the normal distribution, therefore it will be possible to consider as valid the Gaussianity of a dataset in case of  $p \geq 0.05$ .

### III. RESULTS

In this section, the results of the statistical analysis for the four different tests and both PMUs will be presented. Two-hour tests have been considered at each current level. The end of a warm-up period has been waited to guarantee the stationarity of the results.

#### A. PMUs Performance

First, the performance of the PMU is reported in terms of TVE to allow better framing the discussion. Table I shows the maximum TVE values obtained in each test for all the PMUs phases. Both PMUs are clearly compliant with the standard [3], since all the reported values do not exceed the limit of 1%. In particular, PMU 1 is more accurate, with a maximum TVE of 0.086% for phase A in the first test (worst condition), while PMU 2 presents a maximum value of 0.108% in the same test conditions and for the same phase. The two PMUs are both

TABLE I  
MAXIMUM VALUES OF THE CURRENTS' TVE

Test	Maximum TVE [%]					
	PMU 1			PMU 2		
	Phase A	Phase B	Phase C	Phase A	Phase B	Phase C
<b>0.5 A</b>	0.086	0.081	0.075	0.108	0.098	0.097
<b>1.0 A</b>	0.079	0.077	0.071	0.107	0.099	0.095
<b>2.5 A</b>	0.072	0.070	0.065	0.100	0.091	0.088
<b>5.0 A</b>	0.069	0.068	0.065	0.098	0.094	0.090

characterized by a better behavior for increasing current root mean square values.

#### B. Statistical Distributions

The following statistical analysis will consider magnitude and phase-angle contributions separately, and statistical models will be discussed for each of the two quantities.

The magnitude and phase-angle errors of each phase of the two PMUs have been analyzed under the four different test conditions using the S-W statistical tool. As described in Section II-B, every dataset has been adequately decimated following the autocorrelation analysis, which revealed the presence of strongly autocorrelated samples of phase-angle errors for both PMUs, with peaks occurring once every 50 samples. As discussed also in [11], this is not surprising since, when the phase-angle error is dominated by the impact of the synchronization process that typically introduces clock adjustments every second, a recurrent behavior can be expected every 50 samples, corresponding to 1 s at 50 fps.

Tables II and III show the results of the Gaussianity tests in terms of  $p$  for PMU 1 and PMU 2, respectively. As mentioned above,  $p \geq 0.05$  can be recognized as a signature of Gaussian distribution. S-W test outcomes thus state that the null hypothesis cannot be rejected for the majority of the

TABLE II  
SHAPIRO-WILK TEST RESULTS FOR PMU 1

Test	Sample size	p-value from Shapiro-Wilk test					
		Magnitude Error			Phase-Angle Error		
		Phase A	Phase B	Phase C	Phase A	Phase B	Phase C
<b>0.5 A</b>	<b>3000</b>	0.98	1.00	1.00	1.00	1.00	0.98
	<b>1000</b>	1.00	1.00	1.00	1.00	1.00	1.00
	<b>500</b>	1.00	1.00	1.00	1.00	1.00	1.00
	<b>100</b>	1.00	1.00	1.00	1.00	1.00	1.00
<b>1.0 A</b>	<b>3000</b>	1.00	0.99	1.00	0.98	0.91	0.87
	<b>1000</b>	1.00	1.00	1.00	1.00	1.00	1.00
	<b>500</b>	1.00	1.00	1.00	1.00	1.00	1.00
	<b>100</b>	1.00	1.00	1.00	1.00	1.00	1.00
<b>2.5 A</b>	<b>3000</b>	0.74	1.00	1.00	0.19	0.32	0.11
	<b>1000</b>	1.00	1.00	1.00	0.43	0.46	0.42
	<b>500</b>	1.00	1.00	1.00	0.92	0.87	0.63
	<b>100</b>	1.00	1.00	1.00	1.00	0.98	1.00
<b>5.0 A</b>	<b>3000</b>	0.99	0.99	0.99	0.29	0.29	0.13
	<b>1000</b>	1.00	1.00	0.99	0.75	0.51	0.39
	<b>500</b>	0.94	1.00	1.00	0.37	0.32	0.34
	<b>100</b>	1.00	1.00	1.00	0.90	0.91	0.89

TABLE III  
SHAPIRO-WILK TEST RESULTS FOR PMU 2

Test	Sample size	p-value from Shapiro-Wilk test					
		Magnitude Error			Phase-Angle Error		
		Phase A	Phase B	Phase C	Phase A	Phase B	Phase C
0.5 A	3000	1.00	0.99	0.99	0.00	0.00	0.00
	1000	1.00	1.00	1.00	0.08	0.00	0.06
	500	1.00	1.00	1.00	0.23	0.15	0.25
	100	1.00	1.00	1.00	0.99	1.00	1.00
1.0 A	3000	0.52	0.99	0.97	0.00	0.00	0.00
	1000	0.99	1.00	1.00	0.00	0.00	0.00
	500	0.99	1.00	1.00	0.00	0.00	0.00
	100	1.00	1.00	1.00	0.08	0.09	0.07
2.5 A	3000	1.00	0.96	0.99	0.00	0.00	0.00
	1000	1.00	1.00	1.00	0.00	0.00	0.00
	500	1.00	1.00	1.00	0.00	0.00	0.00
	100	1.00	1.00	1.00	0.00	0.00	0.00
5.0 A	3000	0.97	0.94	0.93	0.00	0.00	0.00
	1000	0.99	0.98	0.99	0.00	0.00	0.00
	500	1.00	1.00	1.00	0.00	0.00	0.00
	100	1.00	1.00	1.00	0.00	0.00	0.00

considered case studies. PMU 1 shows a Gaussian behavior for all the three phases, both in magnitude and phase-angle errors, and in each one of the four performed tests.

Coherently with the results found during the autocorrelation analysis, small decimation factors are used for magnitude errors, whereas phase-angle errors show Gaussianity when higher decimation factors are considered. PMU 2 phase-angle errors are almost always incompatible with Gaussian distribution and this is better clarified by the error histograms.

Figures 3-10 show the histograms obtained from decimated data of both PMUs when 1000-size vectors are considered (superimposed fitted normal density is also shown in Figs. 3-9). Only phase A results are reported, but similar considerations apply to the other phases.

The magnitude error histograms of PMU 1 are reported in Figs. 3 and 5 for the tests at 0.5 A and 5.0 A, respectively, while the corresponding histograms for PMU 2 are in Figs. 7

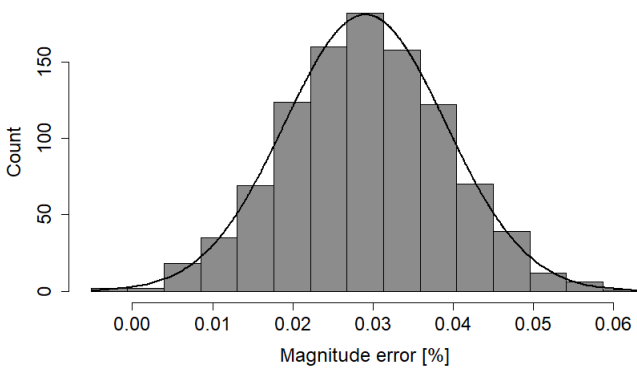


Fig. 3. Histogram of magnitude errors for PMU 1 phase A: 0.5 A test.

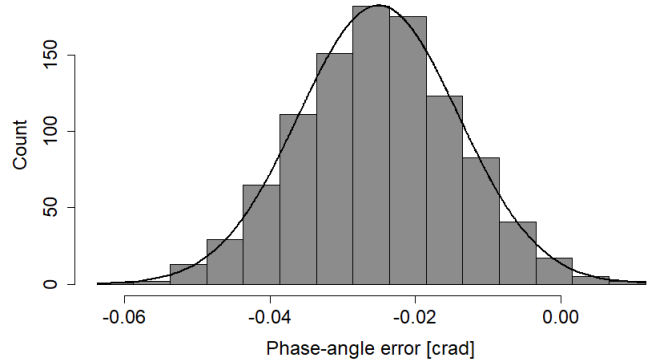


Fig. 4. Histogram of phase-angle errors for PMU 1 phase A: 0.5 A test.

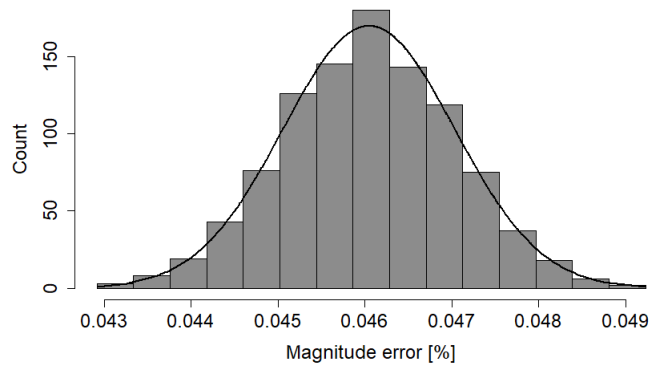


Fig. 5. Histogram of magnitude errors for PMU 1 phase A: 5.0 A test.

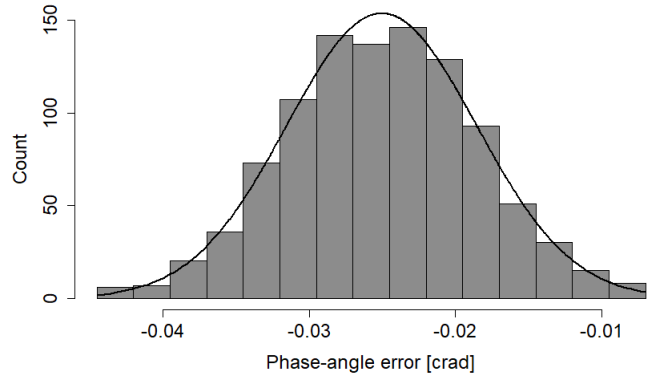


Fig. 6. Histogram of phase-angle errors for PMU 1 phase A: 5.0 A test.

and 9. They all confirm the Gaussian model found with the S-W test. More variegate are instead phase-angle error histograms.

Figures 4 and 6 show a Gaussian-like behavior of the data from PMU 1 for 0.5 A and 5.0 A, respectively, and they

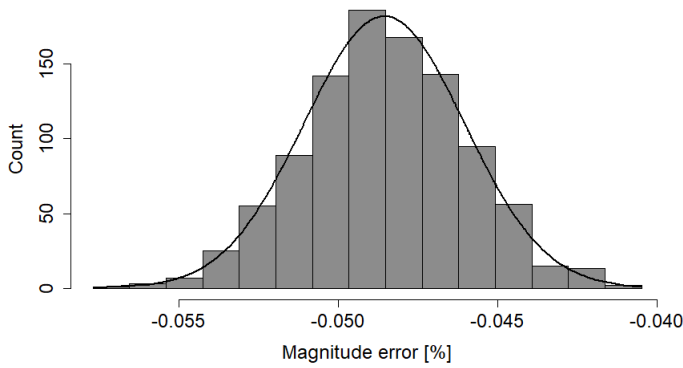


Fig. 7. Histogram of magnitude errors for PMU 2 phase A: 0.5 A test.

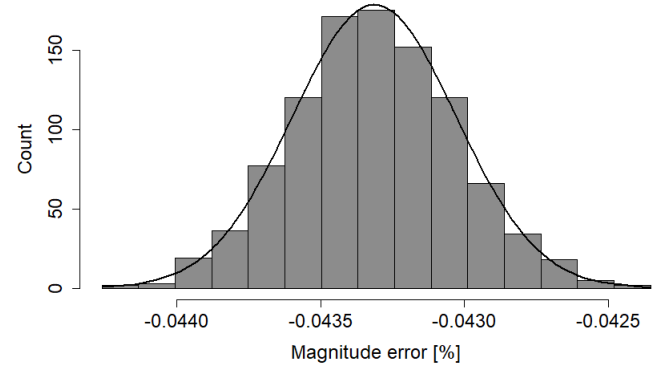


Fig. 9. Histogram of magnitude errors for PMU 2 phase A: 5.0 A test.

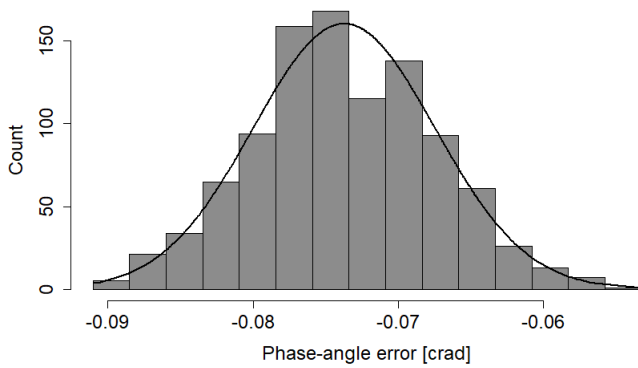


Fig. 8. Histogram of phase-angle errors for PMU 2 phase A: 0.5 A test.

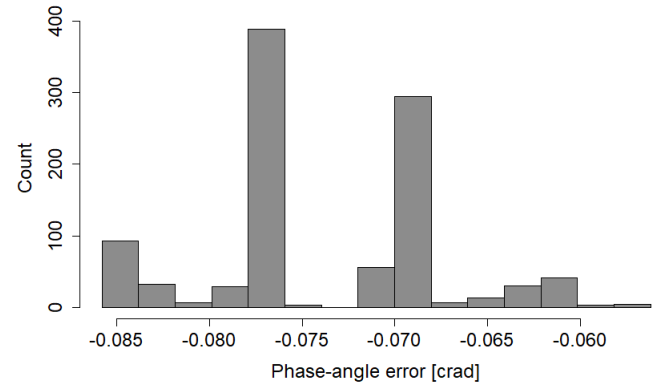


Fig. 10. Histogram of phase-angle errors for PMU 2 phase A: 5.0 A test.

reflect S-W findings (see Table II, sample size 1000). When looking at Fig. 8, which shows phase-angle error histogram for PMU 2 at 0.5 A, Gaussian distribution is still an option even though deviations from normality appear (and they are indeed confirmed by Table III results when 3000 samples are considered). Instead, Fig. 10 confirms the clearly non-Gaussian behavior of phase-angle errors at a higher current level. The errors appear to be located at almost discrete levels, thus highlighting mechanisms similar to those discussed in [11] about synchronization impact. This behavior of PMU 2 phase angles appears more evident as the current level increases, manifesting itself even for 100-size vectors, as shown in Table III.

#### IV. CONCLUSIONS

This paper has presented a characterization of the current magnitude and phase-angle errors of PMU measurements aimed at defining statistical error models. Two commercial PMUs have been tested in a controlled environment under steady-state conditions, avoiding the misleading statistics that can arise from correlated or non-stationary signals. The analysis reveals that the Gaussian distribution is often a good choice,

in particular for magnitude errors, regardless the current level. Phase-angle errors might be affected by more complex dynamics related to the synchronization system that, when phase-angle measurements are accurate, might represent the prevailing error contribution. The analysis conducted in this paper might be applied in further studies on other quantities measured by PMUs or extended to increase awareness of the behavior of the devices under test in different operating conditions.

#### REFERENCES

- [1] P. Castello, M. Lixia, C. Muscas, and P. A. Pegoraro, "Impact of the model on the accuracy of synchrophasor measurement," *IEEE Transactions on Instrumentation and Measurement*, vol. 61, no. 8, pp. 2179–2188, 2012.
- [2] P. Castello, P. Ferrari, P. Pegoraro, and S. Rinaldi, "Chapter 5 - Hardware for PMU and PMU integration," in *Phasor Measurement Units and Wide Area Monitoring Systems*, A. Monti, C. Muscas, and F. Ponci, Eds. Academic Press, 2016, pp. 63–86.
- [3] "IEC/IEEE international standard - measuring relays and protection equipment - part 118-1: Synchrophasor for power systems - measurements," *IEC/IEEE 60255-118-1:2018*, pp. 1–78, 2018.
- [4] S. Brahma, R. Kavasseri, H. Cao, N. R. Chaudhuri, T. Alexopoulos, and Y. Cui, "Real-time identification of dynamic events in power systems using PMU data, and potential applications—models, promises, and

- challenges,” *IEEE Transactions on Power Delivery*, vol. 32, no. 1, pp. 294–301, 2017.
- [5] C. Muscas, P. A. Pegoraro, S. Sulis, M. Pau, F. Ponci, and A. Monti, “New Kalman filter approach exploiting frequency knowledge for accurate PMU-based power system state estimation,” *IEEE Transactions on Instrumentation and Measurement*, vol. 69, no. 9, pp. 6713–6722, 2020.
- [6] P. A. Pegoraro, K. Brady, P. Castello, C. Muscas, and A. von Meier, “Compensation of systematic measurement errors in a PMU-based monitoring system for electric distribution grids,” *IEEE Transactions on Instrumentation and Measurement*, vol. 68, no. 10, pp. 3871–3882, 2019.
- [7] C. Huang, C. Thimmisetty, X. Chen, E. Stewart, P. Top, M. Korkali, V. Donde, C. Tong, and L. Min, “Power distribution system synchrophasor measurements with non-gaussian noises: Real-world data testing and analysis,” *IEEE Open Access Journal of Power and Energy*, vol. 8, pp. 223–228, 2021.
- [8] F. Aminifar, M. Shahidehpour, M. Fotuhi-Firuzabad, and S. Kamalinia, “Power system dynamic state estimation with synchronized phasor measurements,” *IEEE Transactions on Instrumentation and Measurement*, vol. 63, no. 2, pp. 352–363, 2014.
- [9] M. Ajoudani, A. Shiekholeslami, and A. Zakariazadeh, “Improving state estimation accuracy in active distribution networks by coordinating real-time and pseudo-measurements considering load uncertainty,” *IET Generation, Transmission & Distribution*, vol. 16, no. 8, pp. 1620–1638, 2022.
- [10] S. Wang, J. Zhao, Z. Huang, and R. Diao, “Assessing gaussian assumption of PMU measurement error using field data,” *IEEE Transactions on Power Delivery*, vol. 33, no. 6, pp. 3233–3236, 2018.
- [11] P. Castello, C. Muscas, and P. A. Pegoraro, “Statistical behavior of PMU measurement errors: An experimental characterization,” *IEEE Open Access Journal of Instrumentation and Measurement*, vol. 1, pp. 1–9, 2022.
- [12] A. Pal, P. Chatterjee, J. S. Thorp, and V. A. Centeno, “Online calibration of voltage transformers using synchrophasor measurements,” *IEEE Transactions on Power Delivery*, vol. 31, no. 1, pp. 370–380, 2016.
- [13] P. A. Pegoraro, C. Sitzia, A. V. Solinas, and S. Sulis, “PMU-based estimation of systematic measurement errors, line parameters, and tap changer ratios in three-phase power systems,” *IEEE Transactions on Instrumentation and Measurement*, vol. 71, pp. 1–12, 2022.
- [14] L. Yang, P. A. Crossley, A. Wen, R. Chatfield, and J. Wright, “Design and performance testing of a multivendor IEC61850–9-2 process bus based protection scheme,” *IEEE Transactions on Smart Grid*, vol. 5, no. 3, pp. 1159–1164, 2014.
- [15] “IEEE Standard for synchrophasor data transfer for power systems,” *IEEE Std C37.118.2-2011 (Revision of IEEE Std C37.118-2005)*, pp. 1–53, 2011.
- [16] “IEEE Standard profile for use of IEEE 1588 precision time protocol in power system applications,” *IEEE Std C37.238-2017 (Revision of IEEE Std C37.238-2011)*, pp. 1–42, 2017.
- [17] Posit team, *RStudio: Integrated Development Environment for R*, Posit Software, PBC, Boston, MA, 2022. [Online]. Available: <http://www.posit.co/>
- [18] S. S. Shapiro and M. B. Wilk, “An analysis of variance test for normality (complete samples),” *Biometrika*, vol. 52, no. 3/4, pp. 591–611, 1965.